Microchimica Acta
https://doi.org/10.1007/s00604-018-3067-0

ORIGINAL PAPER

A competitive colorimetric chloramphenicol assay based on the non-cross-linking deaggregation of gold nanoparticles coated with a polyadenine-modified aptamer

Yuanyang Xie[1,2] · Yu Huang[1] · Dongyun Tang[1] · Hongliang Cui[1] · Haiyan Cao[3]

Received: 3 August 2018 / Accepted: 20 October 2018

Abstract

A competitive colorimetric assay has been established to detect chloramphenicol (CAP). It is based on the use of colloidal and electrostatically stabilized aptamer-modified gold nanoparticles (GNPs). The CAP aptamer is modified by a sequence of 5 adenosine groups to anchor it on the surface of GNPs. It can competitively capture two compounds, viz. D-(-)-threo-2-amino-1-(4-nitrophenyl)-1,3-propanediol (CAP-base, with a positive charge) and CAP (which is uncharged). The capture of the positively charged CAP-base triggers the aggregation of modified GNPs in salt-containing solution, and this causes a color change from red to purple. However, in the presence of CAP and CAP-base, the capture of the uncharged CAP weakens this color change by a competing process for capture. Thus, the concentration of CAP is associated with the degree of deaggregation of GNPs and can be quantified by the ratio of absorbances at 620 nm and 520 nm. The assay has a 22 nM limit of detection in acidic solution, and the response is linear in the range of 0.20 to 3.20 μM CAP concentration. This assay was successfully applied to the determination of CAP in spiked environmental water samples. Conceivably, this method has a wide scope in that it may be applied to a wide range of analytes if respective aptamers are available.

Keywords D-(-)-threo-2-amino-1-(4-nitrophenyl)-1,3-propanediol · Surface charge · Water analysis

Introduction

Gold nanoparticles (GNPs) have super sensitivity for the change of surrounding environment due to their localized surface plasmon resonance (LSPR) [1]. Thus, GNP-based colorimetric assays have attracted considerable attention in a broad range of field [2]. The non-cross-linking aggregating/dispersing colorimetric probe (NACP) based on the single-stranded-DNA-functionalized GNPs (ssDNA@GNPs) is a significant branch in GNP-based assay [3, 4]. Compared with cross-linking probe, it is simpler due to the usage avoidance of mediation designed to cross link [5]. Furthermore, the ssDNA modified special groups, such as thiol and poly adenines (polyA), are firmly immobilized on the surface of GNPs, rather than the weak forces provided by unmodified ssDNA absorbing on GNPs [6–8]. Hence, the GNPs functionalized by modified ssDNA (m-ssDNA@GNPs) have a higher degree of stabilization than the GNPs cooperating with the unmodified ssDNA. The signal of assay based on m-ssDNA@GNPs is originated from the modification of properties of targets captured by the ssDNA or the changing structure of ssDNA after the capture of targets. Based on this methodology, Maeda et al. established an aggregating direct assay, and Zhao et al. proposed a deaggregating direct assay [6, 9]. Both of their assays have an excellent performance in detecting targets. However, in direct assay, the signal will be weak if the properties of target are too soft to impact the GNPs. Fortunately, the indirect assay, such as competitive assays, based on m-ssDNA@GNPs

Yuanyang Xie and Yu Huang contributed equally to this work.

Electronic supplementary material The online version of this article (https://doi.org/10.1007/s00604-018-3067-0) contains supplementary material, which is available to authorized users.

✉ Yu Huang
huangyu@cigit.ac.cn

✉ Haiyan Cao
513923170@qq.com

[1] Chongqing Institute of Green and Intelligent Technology, Chinese Academy of Sciences, Chongqing 400714, China

[2] University of Chinese Academy of Science, Beijing 100049, China

[3] School of Chemistry and Chemical Engineering, Yangtze Normal University, Chongqing 408100, China

Published online: 07 November 2018

NACP was rare and can avoid that drawback and extremely expand the application range of NACP.

Chloramphenicol (CAP), the first synthetic antibiotic, has significant status in antibiotic, which has been widely used in clinic, animal husbandry and aquaculture [10]. It is still the first choice for the treatment when patients have severe cephalosporin or penicillin allergy, tetracycline-resistant Vibrio cholera and vancomycin-resistant Enterococcus [11]. However, CAP has been found to cause many diseases, including aplastic anemia, leukemia, bone marrow suppression and gray baby syndrome in the past years, which are extremely risky to human health [12, 13]. Being different from other various analytical methods to detect CAP, such as microbiological assays, enzyme linked immunosorbent assays and the different kinds of chromatographic methods, the colorimetric assay has its unique advantages, including simple, low-cost and easy-operate [14–20].

The aptamer is a kind of ssDNA and selected by the experiential process called the systematic evolution of ligands by exponential enrichment (SELEX) method. It has excellent affinity and specificity for target [3]. It can easily functionalize GNPs to expand the target of ssDNA@GNPs for detection. Taghdisi et al. utilized CAP aptamer as a mediator between GNPs and CAP, and fixed them on the base of well plates to detect CAP [11]. It has an ultra-high sensitivity but the process is complex. Then, Chang et al. established a simpler assay by utilizing unmodified CAP aptamer to protect GNPs from etching [21]. However, the LOD of this method is only 5 μM. Hence, the high efficient competitive assay based on m-ssDNA@GNPs NACP utilizing the CAP aptamer has a potential to be developed for the CAP detection.

In this paper, a simple, low cost and high efficient colorimetric competitive assay based on non-cross-linking deaggregating polyA-aptamer-modified gold nanoparticles is established to detect CAP. By using the SELEX process to select CAP aptamer, the designed aptamer can simultaneously distinguish CAP or the precursor of CAP, D-(-)-threo-2-Amino-1-(4-nitrophenyl)-1,3-propanediol (CAP-base) (Fig. 1) [22]. The CAP aptamer is constantly utilized to anchor on the surface of GNPs and it competitively captured CAP or CAP-base in an acid and high salt environment system. The charge of CAP-base is more positive than that of CAP in acid environment. Due to the negative surface charge of GNPs, the degree of charge of GNPs neutralized by capturing CAP is less than that of CAP-base. Because the CAP aptamer is designed with the addition of AAAAA to 5′, CAP aptamer is firmly immobilized on the surface of GNPs by strong absorption between GNPs and polyA group. This anchored function between GNPs and CAP aptamer enhances the stability of GNPs and decreases the response time of capturing target than that of Au thiol bonds according to the research of Pei et al. [7]. The LOD of CAP detection at 22 nM has been experimentally achieved after 30 min reaction. To the best of our knowledge, this colorimetric competitive assay strategy for the detection of CAP is the first time to apply the theory of electrostatic stabilization in colloid chemistry based on non-cross-linking deaggregation of polyA-aptamer-modified gold nanoparticles. Additionally, this kind of colorimetric assay has tremendous potential to expand their application range in the future based on the properties of targets and the alternation of aptamer.

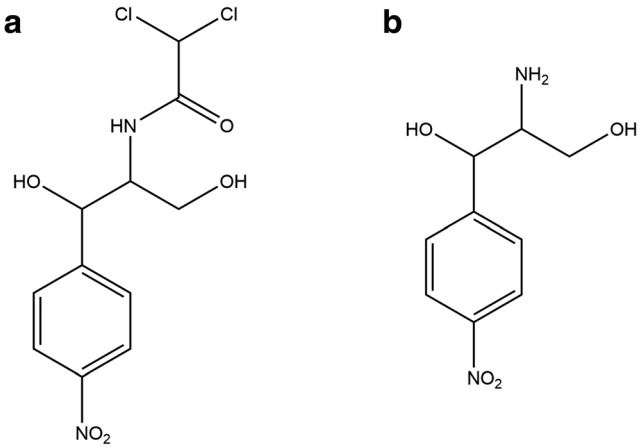

Fig. 1 Chemical structures of **a** chloramphenicol (CAP) and **b** CAP-base – the precursor to CAP, which was used for the selection of CAP aptamer

Materials and methods

Materials

Chloramphenicol (CAP), Thiamphenicol (TAP), kanamycin sulfate (Kana), cephalexin monohydrate (CPX), ampicillin sodium salt (AMP), tetracycline hydrochloride (TC), the 5′-polyA-modified DNA aptamer of CAP (5′-AAAAA *CAA TAA GCG ATG CGC CCT CGC CTG GGG GCC TAG TCC TCT*-3′) [22] and complementary ssDNA of CAP aptamer (5′-AGA GGA CTA GGC CCC CAG GCG AGG GCG CAT CGC TTA TTG-3′) were purchased from Shanghai Biological Technology Development Co., Ltd. (www.sangon.com). D-(-)-threo-2-Amino-1-(4-nitrophenyl)-1,3-propanediol (CAP-base) were purchased from Aladdin (www.aladdin-e.com). Other reagents are given in the Electronic Supporting Material. All reagents were of at least analytical grade and the ultrapure water had resistivity higher than 18 MΩ·cm^{-1} throughout the work.

Apparatus

The UV-Vis absorption spectra were recorded by the custom-made absorption spectroscopy shown in Fig. S1. In the spectroscopy system, the light source was the tungsten halogen lamp (HL-2000-HP, Ocean Optics), and the receiver was the spectrometer (HR4000, Ocean Optics). Then, the 1 cm path-

length quartz cuvette in dark was used as the sample cell and the absorbance from the samples analyzed by programs written in C++ and Matlab. Due to the properties of the spectrometer (HR4000, Ocean Optics) and sample, the acquiring time to record a spectrum from 400 nm to 800 nm was 1 ms. Transmission Electron Microscope (TEM) images were obtained by Zeiss LIBRA 200FEG TEM. The zeta potential was obtained by Malvern Zetasizer Nano ZS.

Preparation of gold nanoparticles

The synthesis of GNPs ~13 nm in diameter was previously described by using sodium citrate reduction method and stored at 4 °C before functionalization [23]. The concentration of GNPs was estimated by Lambert-Beer law, $A = \varepsilon cl$ (the molar extinction coefficient of GNPs at 520 nm was 2.7×10^8 M^{-1} cm^{-1}) [24].

Probe fabrication

The 5′-polyA-modified DNA aptamer functionalized gold nanoparticles (polyA-Apt@GNPs), used as probe, were prepared with referencing of the previous method [7]. Controlling different aptamer/GNPs molar ratio, probes were recorded as polyA-Apt@GNPs (37.5:1), polyA-Apt@GNPs (75:1) and polyA-Apt@GNPs (150:1). Finally, the concentration of polyA-Apt@GNPs was adjusted to be 5.0 nM calculated by extinction coefficient at 520 nm as GNPs.

Assay

The procedure of CAP detection was carried out as follow: polyA-Apt@GNPs were added to the 2 mL solution contained NaCl, acetate buffer, CAP-base and different concentrations of CAP in micro centrifuge tube, shaken thoroughly and incubated 0.5 h at room temperature. The absorption spectra were recorded from 400 nm to 800 nm, and the ratio of absorbance at 620 nm and 520 nm (A_{620nm}/A_{520nm}) was used for quantitative analysis. Then, the concentrations of polyA-Apt@GNPs, NaCl, and CAP-base and the pH value pH of acetate buffer were adjusted to optimize sensitivity of detection. The optimized condition was 0.125 nM polyA-Apt@GNPs, 0.275 M NaCl, 0.01 M acetate buffer (pH 3.0) and 15.0 μM CAP-base after the mixture of solution. The specificity of probes was tested by control experiment using similar compounds.

Analysis of real samples

The real water samples were collected from tap water and Jialing River respectively, and they were filtrated by 0.22 μm PES membrane for purification. Per 1 mL of prepared water samples was mixed with 100 μL of 0.20 M acetate buffer (pH 3.0), 275 μL of 2.0 M NaCl, 100 μL of 0.30 mM CAP-base and 475 μL of ultrapure water in micro centrifuge tube. Then, 50 μL of 5.0 nM polyA-Apt@GNPs (150:1) was added to the mixed solution and incubated 0.5 h at room temperatures before recording the UV-Vis absorption spectroscopy. The spiked water samples were prepared by using 475 μL of CAP solution to replace the same amount of ultrapure water.

Results and discussion

Construction and characterization of polyA-Apt@GNPs colorimetric assay

Figure 2 demonstrates the absorption spectra of GNPs and polyA-Apt@GNPs and the morphology of polyA-Apt@GNPs. After modifying the polyA-modified CAP aptamer by immobilizing polyA on GNPs, the peak of absorption of GNPs red-shifts ~8 nm from 520 nm. According to Kevin et al., the DNA base A has the best relative affinities for gold in four kinds of DNA base and polyA is one of them [25]. Then, the polyA has enough relative affinity to replace the citrate at the surface of GNPs. This immobilization leads the change of refractive index surrounding GNPs and makes their spectra red-shift. Thus, the red-shift of polyA-Apt@GNPs proves that the polyA-modified CAP aptamer was anchored on the surface of GNPs successfully.

It is known that the absorption spectra of polyA-Apt@GNPs are sensitive to the change of local environment and then they are utilized to detect CAP directly and CAP-base. Interestingly, at pH 3.0 and high-salt environment, the signal caused by the change of CAP concentration is unnoticeable while the signal produced by the change of CAP-base concentration is noticeable (Fig. S2). The prevalent aptamer&GNP-based colorimetric assays are based on the presence of targets, which would lead the unmodified aptamer to change their 3D structure and no longer temporarily and weakly adsorbed on GNPs to protect GNPs from salt-induced aggregation [26]. However, the presence of CAP or CAP-base leads to different signal in this assay, which indicates that the immobilization of aptamer on the surface of GNPs is remained even if the target is presence.

Then, based on the different signals between CAP-base and CAP, the polyA-Apt@GNP-based colorimetric competitive assay is established by the competition of CAP aptamer to capture the CAP and CAP-base. The differential absorption ratio of A_{620nm}/A_{520nm} has been chosen for the indication of signal change. The responses to different CAP concentrations with the same CAP-base concentration are illustrated in Fig. 3. The intense aggregation of polyA-Apt@GNPs with only 15 μM CAP-base is obviously observed in the TEM image in Fig. 3. This is the reason for the red-shift of absorption

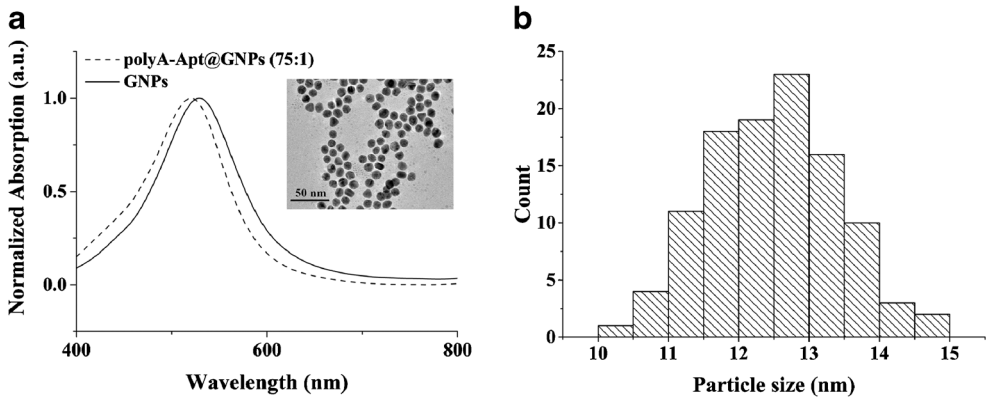

Fig. 2 **a** Normalized absorption spectra of GNPs (dash line) and polyA-Apt@GNPs (75:1) (solid line) (The insert is an enlarged image of polyA-Apt@GNPs (75:1) with diameter of ~13 nm), **b** The histogram of the polyA-Apt@GNPs size in inset TEM image as shown in Fig. 2a

spectra. However, the particles are well dispersed with the addition of CAP. Furthermore, the rapid response time is also observed, which means that the enormous difference between the addition and non-addition of CAP can be distinguished within only 5 min. To obtain the stable signals, 30 min after sample mix was utilized to record the signal.

Optimization of method

The following parameters were optimized: (a) concentration of probe; (b) sample pH value; (c) molar ratio (aptamer/GNPs) of probe; (d) ionic strength; (e) concentration of CAP-base. Relative data and figures are given in the Electronic Supporting Material. The following experimental conditions were found to give best results: (a) concentration of probe: 0.125 nM; (b) sample pH value: 3.0; (c) molar ratio (aptamer/GNPs) of probe: 150:1; (d) ionic strength: 0.275 M NaCl; (e) concentration of CAP-base: 15.0 μM.

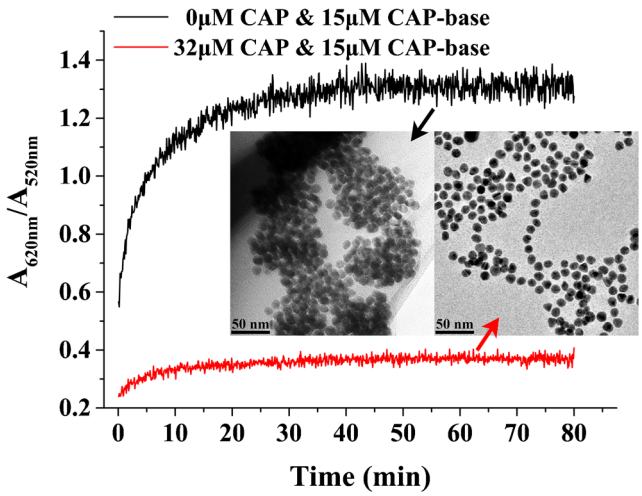

Fig. 3 The responses and TEM images of polyA-Apt@GNPs (75:1) for 0 μM CAP (black line) and 32 μM CAP (red line) at 0.01 M pH 3.0 acetate buffer, 0.2 M NaCl, 15 μM CAP-base and 0.125 nM polyA-Apt@GNPs (75:1)

Detection and specificity of CAP

Under the aforementioned optimized conditions, CAP with different concentration was added respectively and their UV–vis absorption spectra are given in Fig. 4a. With the addition of CAP, the absorption spectra are blue-shift and the full width at half maxima decrease constantly. The color change of corresponding sample can also be observed by bare eyes as shown in the insert of Fig. 4b. The tendency of the corresponding signals, A_{620nm}/A_{520nm} calculated from absorption spectra as the function of CAP concentration, has a monotone decrease first and then tends to be stable at near 0.46 after the addition of 6.00 μM CAP (Fig. 4b). The linear range is between 0.2 μM to 3.2 μM and the equation of fitting linear curve at this part is $A_{620nm}/A_{520nm} = 1.32–0.23 \times c(CAP, \mu M)$ with a coefficient of determination of 0.991. The limit of detection (LOD) of this colorimetric assay was determined to be 22 nM ($S/N = 3$), which is comparable to other reported methods (Table 1). However, this colorimetric detecting strategy does not require high-cost instruments, troublesome enriching processes, time-consuming washing steps and long reacting time, all of which are severe obstacles to on-site monitoring. Additionally, according to related environmental reports, the concentrations of CAP in wastewater of Beijing and municipal sewage of Guiling are 5–36 nM and 18–147 nM respectively [31, 32]. Thus, this strategy for detecting CAP is partly competent for environmental monitoring.

For the specificity of this established colorimetric assay, the 1 mM antibiotics, including TAP, Kana, CPX, AMP and TC were tested respectively under the optimized conditions (Fig. 5). The $\Delta(A_{620nm}/A_{520nm})$ was calculated as the absorption ratio A_{620nm}/A_{520nm} of the blank sample minus that in the presence of antibiotics. The signals of other antibiotics are comparatively slight even if their concentrations are near 420 times more than the concentration of CAP. It demonstrates that the established colorimetric assay has highly specificity.

Moreover, the potential use of this method for real samples was also confirmed by detecting the known quantity of CAP

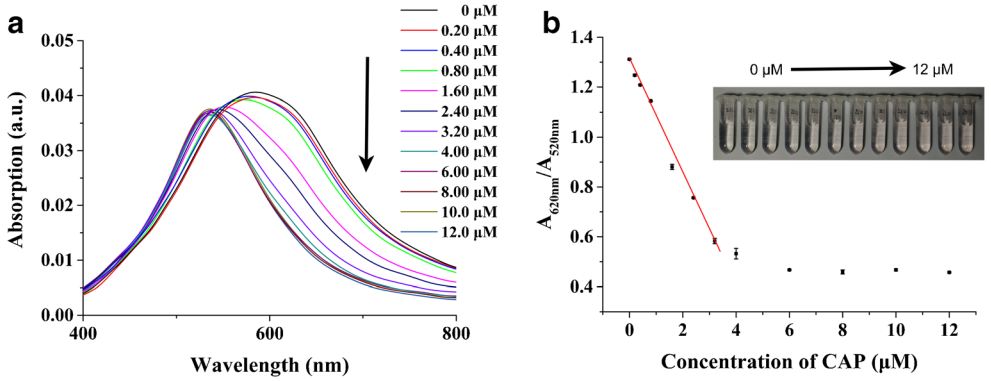

Fig. 4 Highly sensitive performance of the colorimetric competitive assay based on non-cross-linking deaggregating polyA-Apt@GNPs with 0.01 M acetate buffer at pH 3.0, 15.0 μM CAP-base, 0.275 M NaCl and 0.125 nM polyA-Apt@GNPs (150:1). **a** UV–vis absorption spectra of the polyA-Apt@GNPs with different concentrations of CAP. **b** The corresponding signals, A_{620nm}/A_{520nm}, as function of concentrations of CAP. The insert is the corresponding photographs of samples

spiked in tap and river water (Table 2). Each of data is calculated by 3 successive detections. In tap water samples, the recoveries were 80.6%, 87.7% and 96.3% with 5.52%, 3.99% and 2.68% of RSD, corresponding with 0.5, 1.50 and 3.00 μM CAP respectively. In river water samples, the recoveries were 75.4%, 82.7% and 92.2% with 8.46%, 5.30% and 2.87% of RSD, corresponding with 1.50 and 3.00 μM CAP respectively These indicate that this current method for detecting CAP has a good accuracy. However, the detected concentration is lower than the added concentration, and the detected concentration in the river water sample is also lower than that in the tap water sample. It is assumed that the multivalent ion can promote the aggregation of GNPs, which reduces the signal of CAP.

Mechanism of CAP detection

According to Gopinath et al., the surface charge of GNPs plays a key role to impact the aggregation of GNPs and NaCl concentration control is an effective approach to adjust the node point of aggregation [33]. It is noticed that the chemical structural in primary (1°) amine and secondary (2°) amine between CAP-base and CAP is different, which is related to the charge of targets. In the research of Allafchian et al., controlling the pH can vary the charge of cephalexin because of the protonation of primary amine [34]. However, the protonation of secondary amine is harder than that of primary amine. Thus, it is supposed that the protonation of primary of CAP-base make CAP-base has positive charge in an acidic environment. While this using environment is not acidic enough to trigger the protonation of the secondary amine of CAP, which results in the neutral charge of CAP. The capture of targets with different charge impacts the surface charge of polyA-Apt@GNPs and triggers its different degree of aggregation. These different aggregation statuses are corresponding to different direct detection responses between CAP and CAP-base (Fig. S2) and the decease tendency of maximum signals with increasing pH are shown in Fig. S4. Thus, the mechanism that the different signal of polyA-Apt@GNPs in direct detection caused by the different charge status of targets in high-salt environment is supposed, as shown in Scheme 1a.

To further prove the key role of the charge status of target in this detecting strategy, additional experiments were designed, as illustrated in Fig. 6. Compared to the little spectral shifts measured between polyA-Apt@GNPs and CAP at pH 3.0 (Fig. 6a), higher concentration of CAP blue-shifts the spectra of polyA-Apt@GNPs significantly at higher pH (Fig. 6b), which is regarded as the increase in the deaggregating degree of polyA-Apt@GNPs. In contrast, the differential signal measured between polyA-Apt@GNPs and CAP –base at pH 10.0

Table 1 Comparison of the results of different CAP detecting methods

Method	Linear range (μM)	LOD (μM)	Ref.
Voltammetric sensor	0.5–500	0.2	[27]
Amperometric aptasenser	0.01–35	$2*10^{-3}$	[28]
Photoelectrochemical aptasensor	$1.0*10^{-6}$ – $3.0*10^{-3}$	$3.6*10^{-7}$	[29]
Fluorescent aptasensor	10^{-6} - 10^{-2}	$3*10^{-7}$	[30]
Colorimetric aptasensor	10^{-3} - 0.12	$4.15*10^{-4}$	[11]
Colorimetric aptasensor	1–1000	5	[21]
Colorimetric aptasensor	0.2–3.2	0.022	This work

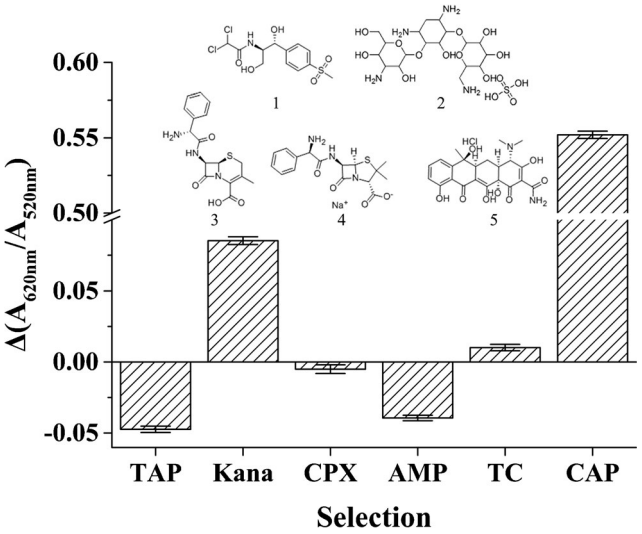

Fig. 5 The specificity test of polyA-Apt@GNPs colorimetric assay with 0.01 M acetate buffer at pH 3.0, 15.0 μM CAP-base, 0.275 M NaCl and 0.125 nM polyA-Apt@GNPs (150:1). The concentrations of other interfering antibiotics were 1 mM and the concentration of CAP was 2.4 μM. The inserts are the structural formulas of TAP, Kana, CPX, AMP and TC (from 1 to 5), respectively

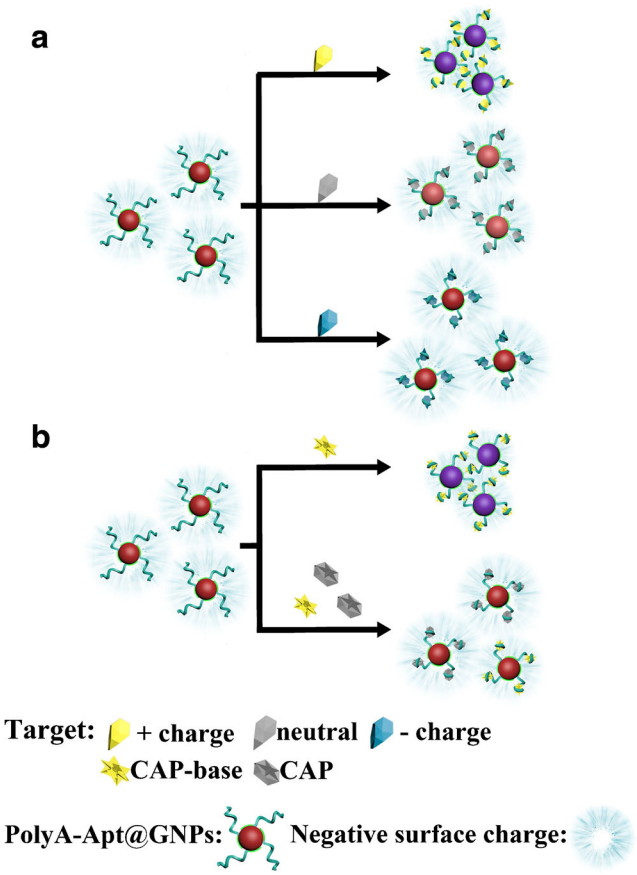

Scheme 1 **a** The respond of polyA-Apt@GNPs detecting targets with different surface charge. **b** The procedure of polyA-Apt@GNPs detecting CAP by the competitive non-cross-linking deaggregating strategy

decreased dramatically (Fig. 6d) compared to that measured at pH 3 (Fig. 6c). This is due to the reduction in the aggregation degree of polyA-Apt@GNPs in the presence of CAP-base at higher pH environment. Thus, increase of pH not only decreases the protonation of primary amine, but promotes the deprotonation of hydroxyl [35]. Based on the proposed mechanism, these results reveal that the charge of CAP is negative and of CAP-base is neutral, which is proved by the appearance of deprotonation of CAP and the disappearance of protonation of CAP-base at high pH. The complementary ssDNA of CAP aptamer is another target of CAP aptamer. After the complement with CAP aptamer, the phosphate groups of the complementary ssDNA expose at outside surface of GNPs could further negative the charge of GNPs in the pH 3.0 based on the K_a of phosphoric acid and deaggregate polyA-Apt@GNPs. The blue-shift of addition of complementary ssDNA in polyA-Apt@GNPs shown in Fig. 6e is in accord with this hypothesis. Because the zeta potential and surface charge is correlated, the zeta potential of the polyA-Apt@GNPs with different concentration of CAP-base at pH 3.0 before the addition of salt to trigger aggregation is shown in Fig. 6f. The consequences are still in accord with the hypothesis that the positive CAP-base decreases the absolute value of zeta potential of polyA-Apt@GNPs.

Finally, based on the mechanism for direct detection, the hypothesis of proposed competitive assay for detecting CAP

Table 2 Performances of colorimetric assay for CAP determination in real water samples ($n = 3$)

Sample number	Sample	Added concentration (μM)	Detected concentration (μM)	Recovery (%)	RSD (%)
1	Tap water	–	–	–	
2	Tap water	0.5	0.40	80.6	5.52
3	Tap water	1.50	1.32	87.7	3.99
4	Tap water	3.00	2.89	96.3	2.68
5	River water	–	–	–	
6	River water	0.5	0.37	75.4	8.46
7	River water	1.50	1.24	82.7	5.30
8	River water	3.00	2.77	92.2	2.87

- CAP was not detected

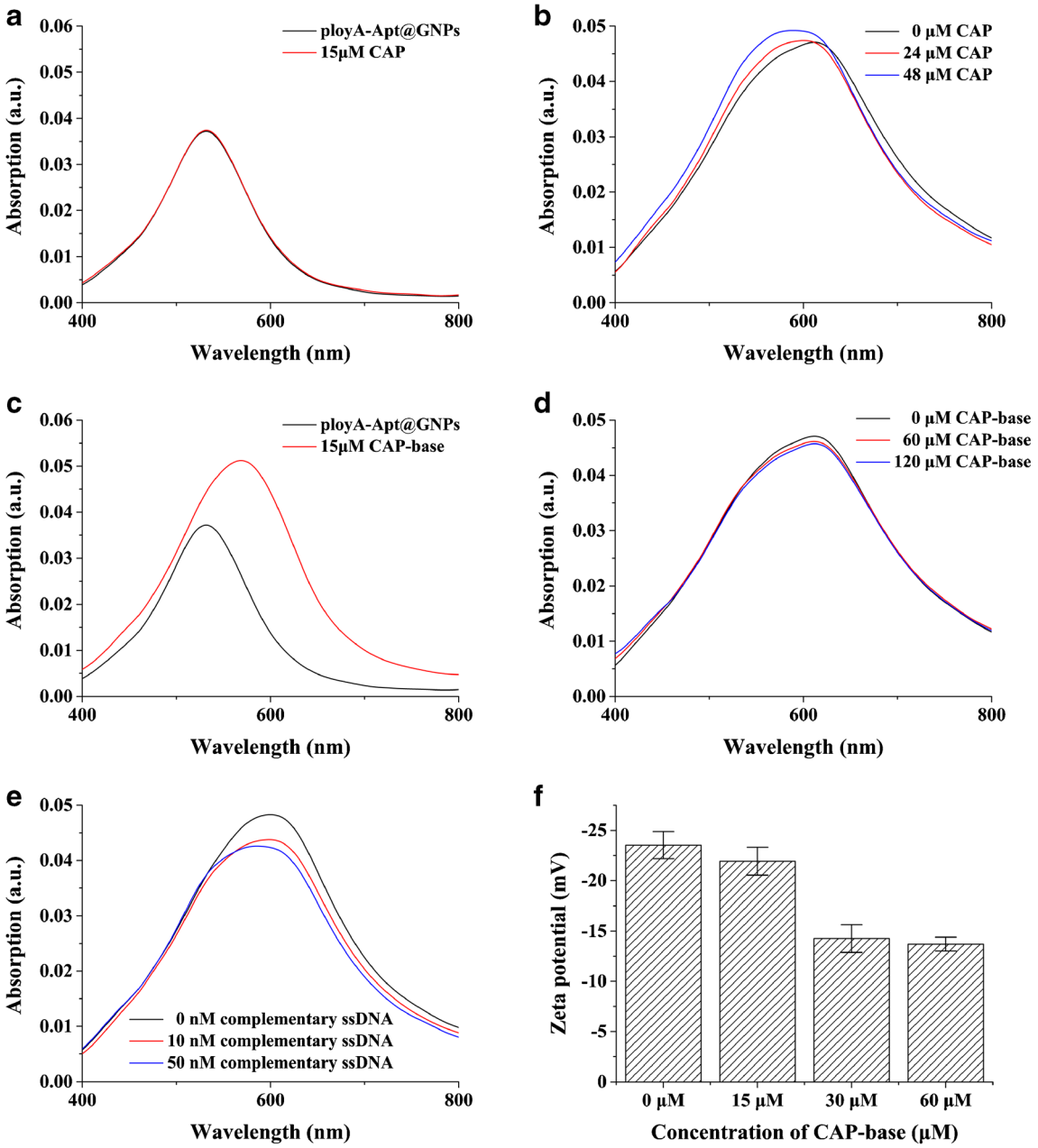

Fig. 6 The exploring experiments for mechanism. UV–vis absorption spectra of the polyA-Apt@GNPs detecting CAP directly in low pH environment (pH 3.0 with 0.125 M NaCl) (**a**) and in high pH environment (pH 10.0 with 0.90 M NaCl) (**b**), and detecting CAP-base directly in low pH environment (**c**) and in high pH environment (**d**). **e** UV–vis absorption spectra of the polyA-Apt@GNPs detecting CAP directly and detecting complementary ssDNA in low pH environment (pH 3.0 with 0.40 M NaCl). **f** The zeta potential of polyA-Apt@GNPs mixed with different concentration of CAP-base in pH 3.0 without NaCl

is depicted in Scheme 1b. The immobilization of CAP or CAP-base on the surface of polyA-Apt@GNPs due to a capture-competition leads them to have different surface charge. Thus, given a constant concentration of CAP-base used, the concentration of CAP would determine the probability of CAP-base captured by polyA-Apt@GNPs. High concentration of CAP can lead small amount of CAP-base to be captured and reduce the aggregation degree of polyA-Apt@GNPs, and vice versa.

Conclusion

An indirect colorimetric assay for detecting CAP based on the competition of CAP aptamer to capture the CAP and CAP-base has been established. Compared with classical GNP-based non-cross-linking aggregation/dispersion colorimetric assay, this method enhances the sensitivity and the toleration degree of salts. Furthermore, the aptamer performed as the recognition unit provides an excellent selectivity. This assay

has been successfully applied in detecting tap water samples and river water samples although the multivalent ion may reduce the detected concentration of CAP. The proposed mechanism indicated that the charge of target play a key role to determine the signals. Therefore, according to electrostatic theory and the easily substituting property of aptamer, this assay has a great potential to expand the target range by altering different kinds of aptamer.

Acknowledgements This work is sponsored by the National Natural Science Foundation of China (Grant No. 21707137), the Key Application and Development Program of Chongqing (No. cstc2017shmsA0159), Natural Science Foundation of Chongqing (Grant No. cstc2018jcyjAX0718), Research Funding Project of Yangtze Normal University (No. 2017KYQD23), Young Scientist Research Fund of Yangtze Normal University, Open Research Fund Program of Key Laboratory of Reservoir Aquatic Environment of CAS.

Compliance with ethical standards The authors declare that they have no competing interests.

References

1. Lee JS, Ulmann PA, Han MS, Mirkin CA (2008) A DNA-gold nanoparticle-based colorimetric competition assay for the detection of cysteine. Nano Lett 8(2):529–533. https://doi.org/10.1021/nl0727563
2. Shahdordizadeh M, Yazdian-Robati R, Ansari N, Ramezani M, Abnous K, Taghdisi SM (2018) An aptamer-based colorimetric lead(II) assay based on the use of gold nanoparticles modified with dsDNA and exonuclease I. Microchim Acta 185(2):151. https://doi.org/10.1007/s00604-018-2699-4
3. Kim YS, Raston NH, Gu MB (2016) Aptamer-based nanobiosensors. Biosens Bioelectron 76:2–19. https://doi.org/10.1016/j.bios.2015.06.040
4. Mirkin CA, Letsinger RL, Mucic RC, Storhoff JJ (1996) A DNA-based method for rationally assembling nanoparticles into macroscopic materials. Nature 382(6592):607–609. https://doi.org/10.1038/382607a0
5. Wang G, Akiyama Y, Shiraishi S, Kanayama N, Takarada T, Maeda M (2017) Cross-linking versus non-cross-linking aggregation of gold nanoparticles induced by DNA hybridization: a comparison of the rapidity of solution color change. Bioconjug Chem 28(1):270–277. https://doi.org/10.1021/acs.bioconjchem.6b00410
6. Zhao W, Chiuman W, Lam JC, McManus SA, Chen W, Cui Y, Pelton R, Brook MA, Li Y (2008) DNA aptamer folding on gold nanoparticles: from colloid chemistry to biosensors. J Am Chem Soc 130(11):3610–3618. https://doi.org/10.1021/ja710241b
7. Pei H, Li F, Wan Y, Wei M, Liu H, Su Y, Chen N, Huang Q, Fan C (2012) Designed diblock oligonucleotide for the synthesis of spatially isolated and highly hybridizable functionalization of DNA-gold nanoparticle nanoconjugates. J Am Chem Soc 134(29):11876–11879. https://doi.org/10.1021/ja304118z
8. Li H, Rothberg L (2004) Colorimetric detection of DNA sequences based on electrostatic interactions with unmodified gold nanoparticles. Proc Natl Acad Sci U S A 101(39):14036–14039. https://doi.org/10.1073/pnas.0406115101
9. Sato K, Hosokawa K, Maeda M (2003) Rapid aggregation of gold nanoparticles induced by non-cross-linking DNA hybridization. J Am Chem Soc 125(27):8102–8103. https://doi.org/10.1021/ja034876s
10. Sai N, Chen Y, Liu N, Yu G, Su P, Feng Y, Zhou Z, Liu X, Zhou H, Gao Z, Ning BA (2010) A sensitive immunoassay based on direct hapten coated format and biotin-streptavidin system for the detection of chloramphenicol. Talanta 82(4):1113–1121. https://doi.org/10.1016/j.talanta.2010.06.018
11. Abnous K, Danesh NM, Ramezani M, Emrani AS, Taghdisi SM (2016) A novel colorimetric sandwich aptasensor based on an indirect competitive enzyme-free method for ultrasensitive detection of chloramphenicol. Biosens Bioelectron 78:80–86. https://doi.org/10.1016/j.bios.2015.11.028
12. Hanekamp JC, Bast A (2015) Antibiotics exposure and health risks: chloramphenicol. Environ Toxicol Pharmacol 39(1):213–220. https://doi.org/10.1016/j.etap.2014.11.016
13. Ding J, Li Q, Xu X, Zhang X, Su Y, Yue Q, Gao B (2018) A wheat straw cellulose-based hydrogel for Cu (II) removal and preparation copper nanocomposite for reductive degradation of chloramphenicol. Carbohydr Polym 190:12–22. https://doi.org/10.1016/j.carbpol.2018.02.032
14. Louie TJ, Tally FP, Bartlett JG, Gorbach SL (1976) Rapid microbiological assay for chloramphenicol and tetracyclines. Antimicrob Agents Chemother 9(6):874–878. https://doi.org/10.1128/aac.9.6.874
15. Chughtai MI, Maqbool U, Iqbal M, Shah MS, Fodey T (2017) Development of in-house ELISA for detection of chloramphenicol in bovine milk with subsequent confirmatory analysis by LC-MS/MS. J Environ Sci Health B 52(12):871–879. https://doi.org/10.1080/03601234.2017.1361771
16. Hussain A, Alajmi MF, Ali I (2016) Determination of chloramphenicol in biological matrices by solid-phase membrane micro-tip extraction and capillary electrophoresis. Biomed Chromatogr 30(12):1935–1941. https://doi.org/10.1002/bmc.3769
17. Luo L, Gu C, Li M, Zheng X, Zheng F (2018) Determination of residual 4-nitrobenzaldehyde in chloramphenicol and its pharmaceutical formulation by HPLC with UV/Vis detection after derivatization with 3-nitrophenylhydrazine. J Pharm Biomed Anal 156:307–312. https://doi.org/10.1016/j.jpba.2018.04.024
18. Chang GR, Chen HS, Lin FY (2016) Analysis of banned veterinary drugs and herbicide residues in shellfish by liquid chromatography-tandem mass spectrometry (LC/MS/MS) and gas chromatography-tandem mass spectrometry (GC/MS/MS). Mar Pollut Bull 113(1–2):579–584. https://doi.org/10.1016/j.marpolbul.2016.08.080
19. Zhang Y, Shao Y, Gao N, Gao Y, Chu W, Li S, Wang Y, Xu S (2018) Kinetics and by-products formation of chloramphenicol (CAP) using chlorination and photocatalytic oxidation. Chem Eng J 333:85–91. https://doi.org/10.1016/j.cej.2017.09.094
20. Miao YB, Gan N, Li TH, Zhang HR, Cao YT, Jiang QL (2015) A colorimetric aptasensor for chloramphenicol in fish based on double-stranded DNA antibody labeled enzyme-linked polymer nanotracers for signal amplification. Sensors Actuators B Chem 220:679–687. https://doi.org/10.1016/j.snb.2015.05.106
21. Chang CC, Wang G, Takarada T, Maeda M (2017) Iodine-mediated etching of triangular gold nanoplates for colorimetric sensing of copper ion and aptasensing of chloramphenicol. ACS Appl Mater Interfaces 9(39):34518–34525. https://doi.org/10.1021/acsami.7b13841
22. Duan Y, Gao Z, Wang L, Wang H, Zhang H, Li H (2016) Selection and identification of chloramphenicol-specific DNA Aptamers by Mag-SELEX. Appl Biochem Biotechnol 180(8):1644–1656. https://doi.org/10.1007/s12010-016-2193-6
23. Liu J, Lu Y (2006) Preparation of aptamer-linked gold nanoparticle purple aggregates for colorimetric sensing of analytes. Nat Protoc 1(1):246–252. https://doi.org/10.1038/nprot.2006.38
24. Liu X, Atwater M, Wang J, Huo Q (2007) Extinction coefficient of gold nanoparticles with different sizes and different capping ligands. Colloids Surf B: Biointerfaces 58(1):3–7. https://doi.org/10.1016/j.colsurfb.2006.08.005

25. Koo KM, Sina AAI, Carrascosa LG, Shiddiky MJA, Trau M (2015) DNA–bare gold affinity interactions: mechanism and applications in biosensing. Anal Methods UK 7(17):7042–7054. https://doi.org/10.1039/c5ay01479d
26. Li X, Cheng R, Shi H, Tang B, Xiao H, Zhao G (2016) A simple highly sensitive and selective aptamer-based colorimetric sensor for environmental toxins microcystin-LR in water samples. J Hazard Mater 304:474–480. https://doi.org/10.1016/j.jhazmat.2015.11.016
27. Sun Y, Wei T, Jiang M, Xu L, Xu Z (2018) Voltammetric sensor for chloramphenicol determination based on a dual signal enhancement strategy with ordered mesoporous carbon@polydopamine and β-cyclodextrin. Sensors Actuators B Chem 255:2155–2162. https://doi.org/10.1016/j.snb.2017.09.016
28. Liu S, Lai GS, Zhang HL, Yu AM (2017) Amperometric aptasensing of chloramphenicol at a glassy carbon electrode modified with a nanocomposite consisting of graphene and silver nanoparticles. Microchim Acta 184(5):1445–1451. https://doi.org/10.1007/s00604-017-2138-y
29. Wang Y, Bian F, Qin X, Wang Q (2018) Visible light photoelectrochemical aptasensor for chloramphenicol by using a TiO2 nanorod array sensitized with Eu(III)-doped CdS quantum dots. Microchim Acta 185(3):161. https://doi.org/10.1007/s00604-018-2711-z
30. Miao YB, Ren HX, Gan N, Zhou Y, Cao Y, Li T, Chen Y (2016) A homogeneous and "off-on" fluorescence aptamer-based assay for chloramphenicol using vesicle quantum dot-gold colloid composite probes. Anal Chim Acta 929:49–55. https://doi.org/10.1016/j.aca.2016.04.060
31. Li J, Shao B, Shen J, Wang S, Wu Y (2013) Occurrence of chloramphenicol-resistance genes as environmental pollutants from swine feedlots. Environ Sci Technol 47(6):2892–2897. https://doi.org/10.1021/es304616c
32. Liu H, Zhang G, Liu CQ, Li L, Xiang M (2009) The occurrence of chloramphenicol and tetracyclines in municipal sewage and the Nanming River, Guiyang City. J Environ Monit 11(6):1199–1205. https://doi.org/10.1039/b820492f
33. Gopinath SC, Lakshmipriya T, Awazu K (2014) Colorimetric detection of controlled assembly and disassembly of aptamers on unmodified gold nanoparticles. Biosens Bioelectron 51:115–123. https://doi.org/10.1016/j.bios.2013.07.037
34. Rayegan A, Allafchian A, Abdolhosseini Sarsari I, Kameli P (2018) Synthesis and characterization of basil seed mucilage coated Fe3O4 magnetic nanoparticles as a drug carrier for the controlled delivery of cephalexin. Int J Biol Macromol 113:317–328. https://doi.org/10.1016/j.ijbiomac.2018.02.134
35. Rimsza JM, Jones RE, Criscenti LJ (2018) Interaction of NaOH solutions with silica surfaces. J Colloid Interface Sci 516:128–137. https://doi.org/10.1016/j.jcis.2018.01.049